Effect of Ferrous (Fe^{2+}) Concentrations on the Rate of Carbon Dioxide (CO_2) Corrosion on X52 Carbon Steel at 50°C and 70°C.

By

Abdul Hanif Bin Abdullah
16102

Dissertation submitted in partial fulfilment of the
requirements for the
Bachelor of Engineering (Hons) (Mechanical)

JANUARY 2016

Universiti Teknologi PETRONAS

Bandar Seri Iskandar

31750 Tronoh Perak Darul Ridzuan

CERTIFICATION OF APPROVAL

Effect of Ferrous (Fe^{2+}) Concentrations on the Rate of Carbon Dioxide (CO_2) Corrosion on X52 Carbon Steel at 50°C and 70°C.

by

Abdul Hanif Bin Abdullah 16102

A project dissertation submitted to the Mechanical Engineering Programme
Universiti Teknologi PETRONAS in partial fulfilment of the requirement for the
BACHELOR OF ENGINEERING (Hons) (MECHANICAL)

Approved by,

_____

(Dr. Saeid Kakooei)

UNIVERSITI TEKNOLOGI PETRONAS

TRONOH, PERAK

January 2016

CERTIFICATION OF ORIGINALITY

This is to certify that I am responsible for the work submitted in this project, that the original work is my own except as specified in the references and acknowledgements, and that the original work contained herein have not been undertaken or done by unspecified sources or persons.

(ABDUL HANIF BIN ABDULLAH)

ABSTRACT

In oil and gas industry, carbon dioxide (CO_2) corrosion is one of the major problem which have caused damages to the pipes and equipment. When CO_2 corrosion occur on low carbon steel, a protective film, called Iron Carbonate ($FeCO_3$) can form when the surrounding parameters are desirable for the formation of film. This film can reduce the rate of CO_2 corrosion. Both rate of CO_2 corrosion and film formation can be affected by Ferrous (Fe^{2+}) Concentration, temperature, pH, etc. Electrochemical experiments were conducted to investigate the effect of Fe^{2+} concentration (0 ppm, 50 ppm and 200 ppm) on the rate of CO_2 corrosion of X52 carbon steel at 50°C and 70°C. The experiments were conducted in solution with pH 6.6 and atmospheric pressure (1 atm) for 48 hours. The rate CO_2 corrosion was measured using Weight Loss Method (WLM), Linear Polarization Resistance (LPR) and Electrochemical Impedance Spectroscopy (EIS). Scanning Electron Microscopy (SEM) and Energy Dispersive Spectroscopy (EDS) was used to analyse the film formation. At the end of the project, Fe^{2+} concentration plays an important role in decreasing the corrosion rate. Temperature is also important to provide a favourable condition for the development of a protective film.

ACKNOWLEDGEMENT

First of all, I am grateful to the Almighty God for giving me patience, strength and guidance throughout this project. I would like to express my gratitude to my supervisor, Dr. Saeid Kakooei for the supervision, suggestions and encouragement that have helped in completing this project. I would also like to thank Dr, Othman Bin Mamat as the examiner for this project.

In addition, many thanks to Mrs. Ain and Mr. Masri from the Corrosion Research Centre (CCR) for their guidance and care especially during the conduction of the corrosion test experiments. Not to forget, Mr. Hafiz, one of the Mechanical Engineering Department technicians that have assisted in the completion of this this project. I would not have succeeded in this project without their assistance. Finally, I would also to express my appreciation to all my friends and family for their support and encouragement.

Table of Contents

LIST OF FIGURES

LIST OF TABLES

ABBREVIATIONS

CO_2 : Carbon Dioxide

$FeCO_3$: Iron Carbonate

Fe^{2+}: Ferrous

WLM : Weight Loss Method

LPR : Linear Polarization Resistance

EIS : Electrochemical Impedance Spectroscopy

SEM : Scanning Electron Microscopy

EDS :Energy Dispersive Spectroscopy

CHAPTER 1: INTRODUCTION

1.1 Background

Carbon steel is widely used as pipes and equipment in oil and gas industry. In this industry, the carbon steel is commonly exposed to excessive environment such as high temperature or pressure, chemicals, stresses and etc. El-Lateef et al. (2012) stated carbon steel is a type of alloy which consists of iron and carbon.

One of the major problems faced by the industry is carbon dioxide (CO_2) corrosion which can also be known as 'sweet corrosion' which usually involves in the upstream operation where the collection fluid or gas takes place. Li et al. (2008) described that CO_2 corrosion on carbon steel is a common problem in the oil industry which results in severe damage to pipes and equipment. Economic loss is the main obstacle by the oil and gas companies due to CO_2 corrosion. Corrosion can result in wastage of material, money, time and man power; cost of replacing corroded structure or components; and total loss of products (Uzorh, 2013).

Li et al. (2008) said that CO_2 gas is corrosive only when it is in an aqueous phase due to its solubility to water and brines where it can cause electrochemical reaction between steel. CO_2 corrosion can be divided into two main forms which are general and localized. Localized corrosion consists of pitting, mesa type attack and flow induced (B. Kermani et al., 2006; Schmitt & Horstemeier, 2006).

A protective film will form when CO_2 corrosion on carbon steel occurs. The dissolution of iron will result in the reaction of ferrous (Fe^{2+}) and carbonate (CO_3^{2-}) to form precipitation of iron carbonate ($FeCO_3$). This precipitates form layer of $FeCO_3$ on the steel surface which act as protective barrier against corrosion. Nesic (2007) stated that the $FeCO_3$film can reduce the rate of corrosion by developing a diffusion barrier for the species involved in the corrosion process and covering the underlying surface. The rate of CO_2corrosion carbon steel is highly dependable on the formation of film under different parameters such as Fe^{2+}concentration, temperature, pressure, pH, etc.

1.2 Problem Statement

CO_2 corrosion on carbon steel is one of the major problems in oil and gas industry. Dissolution of iron (Fe) from carbon steel caused by anodic reaction can form Fe^{2+} which then reacts with $CO_3^{2-}$to form $FeCO_3$ precipitation. This $FeCO_3$ precipitates will form a protective film on the surface of the carbon steel which can reduce the rate of CO_2 corrosion. The rate of CO_2 corrosion carbon steel is highly dependable on the formation of film under different parameters.

Many researchers have done experiments to study the rate of CO_2 corrosion followed by formation of $FeCO_3$ film on carbon steels in different parameters. The researchers used low carbon steels such as X52, X65 and 1020 steel as the samples for the experiments. The researchers found out that the rate of CO_2 corrosion and film formation varies under different parameters (Cabrini et al., 2015; Fang et al., 2013; Sun et al., 2006; Clover et al., 2005; Srdjan Nesic, 2002)

Nesic (2007) mentioned that the peak in the corrosion rate is commonly observed between 60˚C and 80˚C depending on electrolyte conditions. There is no clear research has been done to investigate the rate of CO_2 corrosion and film formation at different Fe^{2+} concentrations at 50°C and 70°C. 50°C and 70°C are the chosen temperatures so that the formation of film can be studied below and between the range temperatures of highest corrosion rate. At the end of the project, the difference of CO_2 corrosion rate and film formation will be compared between the condition at temperature 50°C and 70°C.

1.3 Objectives

i. To study the effect of ferrous (Fe^{2+}) concentrations on the rate of carbon dioxide (CO_2) corrosion on X52 carbon steel at 50°C and 70°C.

1.4 Scope of Study

i. The effect of Fe^{2+} concentration rate of CO_2 corrosion on X52 steel at 50°C and 70°C will be studied by using Weight Loss Method (WLM), Linear Polarization Resistance (LPR) and Electrochemical Impedance Spectroscopy (EIS).

ii. The morphology of film formation on X52 steel surface will be analysed by using Scanning Electron Microscope (SEM) and Energy Dispersive Spectroscopy (EDS).

CHAPTER 2: LITERATURE REVIEW

2.1 Carbon Steel

El-Lateef et al. (2012) stated that carbon steel is a type of alloy which consists of iron and carbon. The carbon will be in iron carbide form which has the high strength and hardness of the carbon steel. Uzorh (2013) explained that elements such as phosphorus, sulphur, silicon and manganese are also contained in the carbon steel which provides certain desirable properties. Carbon steel can be divided into three classes which are low, medium and high carbon steels.

Low carbon steel can be known as mild steel which the carbon content of 0.15%-0.30%.Medium and high carbon steel contain 0.30% - 0.70% and 0.70% - 2.00% of carbon, respectively. Carbon steel is widely used as pipes which play an important role in transportation of gases and liquids over long distance from their source to consumers (El-Lateef et al., 2012). When carbon steel is exposed to water with dissolved CO_2, it will be thermodynamically unstable. Carbon steel is widely used in oil and gas industry because the steel surface can be covered by a protective film of corrosion products.

2.2 Corrosion

Uzorh (2013) defined corrosion as the deterioration or destruction of metal by chemicals and electrochemical reaction by its environment. Metallic corrosion is like a reverse of electroplating where the corroded is the anode while the cathode is that being electroplated. A metal corrodes when it wants to stabilize to return to its stable or nature form. Corrosion has been one of the hardest challenges in maintaining or sustaining operational success in oil and gas industry. This is caused by its impact to the loss of economy and threat to health, safety and environment of people and facilities (B. Kermani et al., 2006).

El-Lateef et al. (2012) stated petroleum and gas pipes are the most common equipment that will face corrosion because of its function to be used for transporting gases or liquid from the reservoir to the surface. Corrosion will result in wastage of material, money, time and man power; cost of replacing corroded structure or components; and

loss of products (Uzorh, 2013). CO_2 corrosion and hydrogen sulphide (H_2S) are the most common types of corrosion that are occur in oil and gas industry (El-Lateef et al., 2012; Tang et al., 2006; B. Kermani et al., 2006; Sun et al., 2006).

2.3 Carbon Dioxide (CO_2) Corrosion

CO_2 corrosion is also known as 'sweet corrosion'. Li et al. (2008) mentioned that CO_2 corrosion can cause damages to the pipes and equipment. This has led to the increase of cost needed in the production of oil and gas due to the loss of production, replacement or maintenance of the damaged equipment. Researchers have been studying this matter since 1940s in developing better understanding of this matter. CO_2 gas is corrosive only when it is in an aqueous phase due to its solubility to water and brines where it can cause electrochemical reaction between steel. However, CO_2 gas is not corrosive in dry phase (M. Kermani & Morshed, 2003). The electrochemical reactions in CO_2 corrosion of steel have been discussed (Dugstad, 2006; El-Lateef et al., 2012; Li et al., 2008; Nesic, 2007).

Equation (1) shows the reaction when CO_2 is dissolved in water (H_2O), it forms carbonic acid (H_2CO_3).

$$CO_2 + H_2O \rightarrow H_2CO_3 \qquad (1)$$

H_2CO_3 will then go through cathodic reaction while Fe will go through anodic reaction. Equation (2) shows the anodic reaction of Fe to form Fe^{2+}.

$$Fe \rightarrow Fe^{2+} + 2e^{-} \qquad (2)$$

Equations (3) and (4) show the further electrochemical cathodic processes connected with the direct reduction of H_2CO_3 and bicarbonate (HCO_3^-).

$$2H_2CO_3 + 2e^- \rightarrow H_2 + 2HCO_3^- \quad (3)$$

$$2HCO_3^- + 2e^- \rightarrow 2CO_3^{2-} + 2H^+ \quad (4)$$

Equation (5) shows the cathodic reaction of hydrogen ions (H^+) to form hydrogen (H_2) gas.

$$H^+ + 2e^- \rightarrow H_2 \quad (5)$$

Equation (6) shows the reaction between Fe^{2+} and CO_3^{2-} to form $FeCO_3$ precipitate.

$$Fe^{2+} + CO_3^{2-} \rightarrow FeCO_3 \quad (6)$$

Equation (7) shows the overall reaction, where the final products are $FeCO_3$ and H_2 gas.

$$Fe + CO_2 + H_2O \rightarrow FeCO_3 + H_2 \quad (7)$$

2.4 Forms Of Carbon Dioxide (CO_2) Corrosion Damage

There are two main forms of CO_2corrosion which are general and localised corrosion. (B. Kermani et al., 2006; Schmitt & Horstemeier, 2006).

2.4.1 General Corrosion

B. Kermani et al. (2006) mentioned that general corrosion is also known as uniform corrosion. This type of corrosion happens uniformly over the steel surface either by chemical reaction or electrochemical reaction. This leads to relatively uniform thinning on the steel surface.

2.4.2 Localised Corrosion

B. Kermani et al. (2006) stated that localised corrosion consists of three forms which are pitting, mesa type attack and flow induced.

2.4.2.1 Pitting

Pitting corrosion can happen in a gas-producing well with low velocities and around the dew-point temperatures. It occurs under relatively stagnant conditions and there is no rule of thumb to assume when such attack will occur. This type of corrosion will cause holes or cavities to form beneath the material surface. Pitting corrosion is difficult to be detected when and where it happens due to the corrosion products that covers the pits. Therefore, pitting corrosion is expected to be destructive than general corrosion. Moreover, even though pitting corrosion causes low amount of material loss on the surface, it eventually causes more damage to the inner structure of the material. (B. Kermani et al., 2006).

2.4.2.2 Mesa Type Attack

Mesa type attack is commonly happen in young gas wells with high pressure or acid gases. It occurs in low to medium flow conditions where $FeCO_3$ film can form, but it is unstable which leads to the removal of the film. The damaged film is caused by the shear force produced by the gas travelling under the surface. The removal of the film exposed the steel to further corrosion. Mesa type attack is appeared to be less sensitive to the velocity of fluid but it is dependent to fluid composition. In identifying this mesa type attack, it usually appears in the form of holes with sharp edges (B. Kermani et al., 2006; M. Kermani & Morshed, 2003).

2.4.2.3 Flow Induced

Flow induced corrosion usually occurs in high flow conditions where the corrosion starts in the form of pits of mesa attack above critical flow intensities. Local turbulence created by the pits at the mesa attack or bulging geometry can propagate flow induced corrosion. The present protective film might be destroyed when the local turbulence combined with the stresses produced in the formation of film. The flow conditions prevent the reformation of protective film on the exposed surface when the film is destroyed or damaged (B. Kermani et al., 2006; M. Kermani & Morshed, 2003).

2.5 Mechanism of Film Formation

Dugstad (2006) stated that when CO_2 corrosion, carbon steel can be damaged and thus losing its properties which can lead to loss of equipment overtime. Even though, CO_2 gas is harmful, it can actually form a protective film on the steel surface that can decrease the rate of corrosion. This protective film is known as $FeCO_3$ film. Equation (6) shows the formation of $FeCO_3$ precipitate Fe^{2+} and CO_3^{2-} concentrations have exceeded the saturation level. The precipitates will then form $FeCO_3$ film that can reduce the rate of corrosion by developing a barrier that covers the underlying surface against species that involved in corrosion process (Nesic, 2007; Srdjan Nesic, 2002; Sun et al., 2006).

As stated by Dugstad (2006), the mainspring for precipitation is the supersaturation of $FeCO_3$. A high degree of supersaturation of $FeCO_3$ is required in order to get sufficient amount of $FeCO_3$ to form on the steel. Supersaturation (S) can be calculated

by using equation (8), where $C_{Fe^{2+}}$ and $C_{CO_3^{2-}}$ corresponds to concentration of Fe^{2+} and CO_3^{2-}; and K_{sp} is the solubility product for $FeCO_3$ (Nesic, 2007; Nesic, Wang, Cai, & Xiao, 2004; Srdjan Nesic, 2002).

$$S = \frac{C_{Fe^{2+}} + C_{CO_3^{2-}}}{K_{sp}} \qquad (8)$$

Li et al. (2008) mentioned there are three layers of film involved in the formation of a very protective $FeCO_3$ film. The first layer form is called the outer layer. This is the early stage where the $FeCO_3$ will start to precipitate in the form of cube crystals at the steel surface which decreases the rate of corrosion by presenting a barrier that blocks a portion of steel surface. Eventually, the steel surface below will continuously corrode and forms 'voids' between the film and the steel surface.

As mentioned by Li et al. (2008), CO_3^{2-} and HCO_3^- could go through the outer layer because the layer is not compact due to porosity. These ions will react with the underlying steel surface. The $FeCO_3$ formed underneath the outer layer will construct a middle layer consist of dendritic structure. At this stage, the outer layer will crack due to the increase of stress in the middle layer. This shows that the middle layer start to become more compact.

Even though the middle layer is more compact to the outer layer, CO_3^{2-} and HCO_3^- can steel penetrate and react with the steel surface. This reaction causes $FeCO_3$ to precipitate beneath the middle layer and thus forming denser and more compact crystalline layer which is called the inner layer (Li et al., 2008).

2.6 The Effect Of Parameters On The Rate Of CO_2 Corrosion And Film Formation

2.6.1 The effect of Fe^{2+}concentration

As stated by Tanupabrungsun, Brown, and Nesic (2013), the rate of $Fe^{2+}$and CO_3^{2-} to form $FeCO_3$ precipitate is related to the rate of formation of $FeCO_3$ on the metal surface. The degree of supersaturation can reflect the rate of precipitation as described in Equation (8). Srdjan Nesic (2002) conducted an experiment to illustrate the effect of Fe^{2+} concentration on the rate of CO_2 corrosion on carbon steel. Fig. 1 and 2 show the results of film thickness, porosity and corrosion rate obtained with different Fe^{2+} concentrations of 5 ppm, 25 ppm, 100 ppm and 250 ppm.

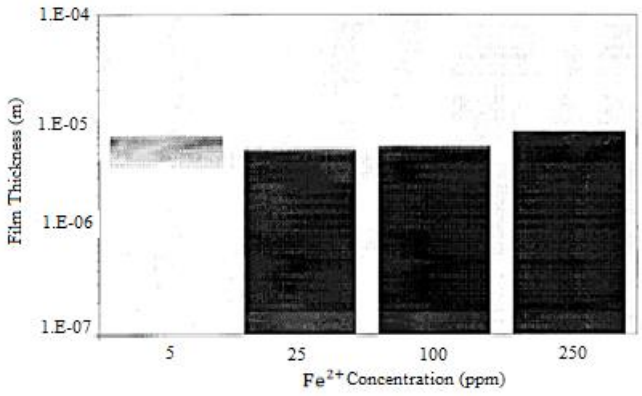

FIGURE 1: Chart of Film Thickness and Porosity against Fe^{2+} Concentration

(Srdjan Nesic, 2002)

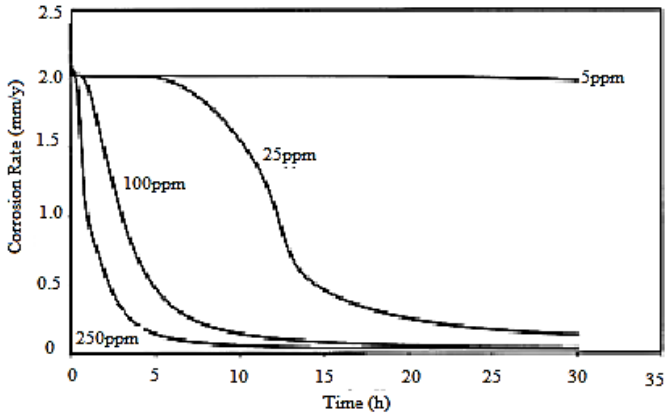

FIGURE 2: Graph of Corrosion Rate against Time at Different Fe^{2+}Concentrations

(Srdjan Nesic, 2002)

The film formed at Fe^{2+} concentration of 5 ppm was very less protective and high in porosity which did not reduce the corrosion rate. At 25 ppm, a dense and thick film was formed. The density and thickness of films increased as the Fe^{2+}concentration increased. Corrosion rate at Fe^{2+} concentration of 250 ppm was reduced faster compared to 100 ppm and 25 ppm due to denser and thicker protective film.

2.6.2 The effect of temperature

According to Li et al. (2008),the best temperature for the growth of $FeCO_3$ film is at 65°C. Cabrini et al. (2015) mentioned that at temperature lower than 60°C,the film was more porous and less protective. Srdjan Nesic et al. (2002) conducted experiments on carbon steel with different temperatures of 50˚C, 55˚C, 65˚C and 80˚C. Fig. 3 and Fig.4 show the thickness and porosity of film, and the effect to the rate of CO_2 corrosion at different temperatures.

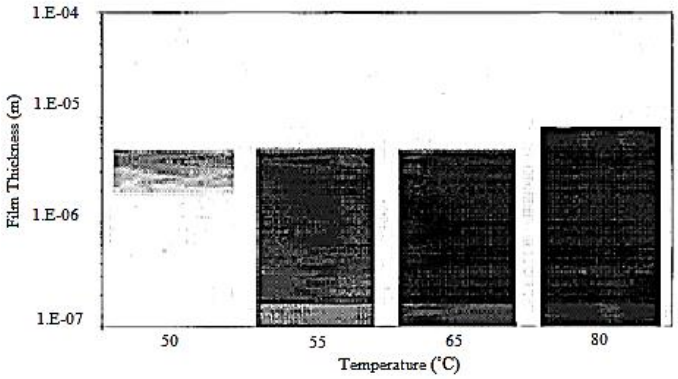

FIGURE 3: Chart of Film Thickness and Porosity against Temperature

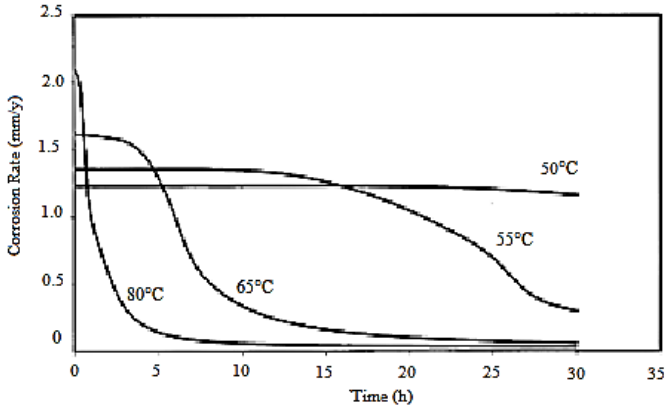

FIGURE 4: Graph of Corrosion Rate against Time at Different Temperatures

The results showed that very protective films were formed at 55°C, 65°C and 80°C,while at 50°C very porous film was be detected. It is clear that difference of 5°C two very different corrosion outcomes. The film formed at 55°C was more porous as compared to film formed at 65°C.A very dense and thick protective film was obtained at 80°C which greatly decreased the rate of CO_2 corrosion. Nesic (2007) mentioned that the peak in the corrosion rate is commonly observed between 60˚C and 80˚C depending on electrolyte conditions.

2.6.1 The effect of pH

pH can affect the corrosion rate of carbon steels in both electrochemical reactions that lead to iron dissolution and the precipitation of protective film. As the pH increases, the formation of protective film also increases which lead to denser and more protective film. To illustrate this, experimental results from Srdjan Nesic (2002) explain the relationship of carbon steel under the pH of 5.8, 6.0, 6.26 and 6.6. The experiment was conducted at temperature of 80°C, CO_2 partial pressure of 0.54 bar, Fe^{2+} concentration of 250 ppm and velocity of lm/s. Fig. 2 and 3 shows the film thickness and porosity; and corrosion rate as a function of pH.

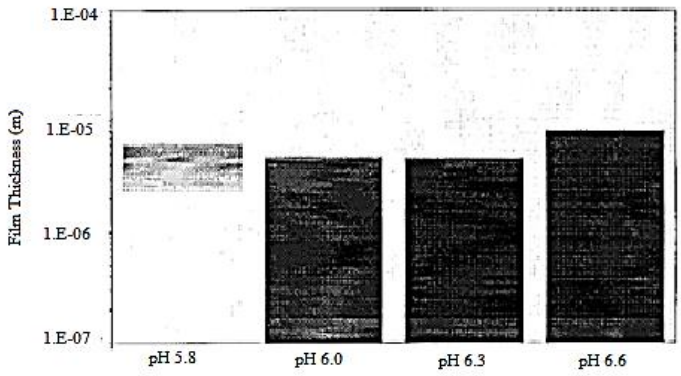

FIGURE 5: Chart of film thickness and porosity against pH (Srdjan Nesic, 2002)

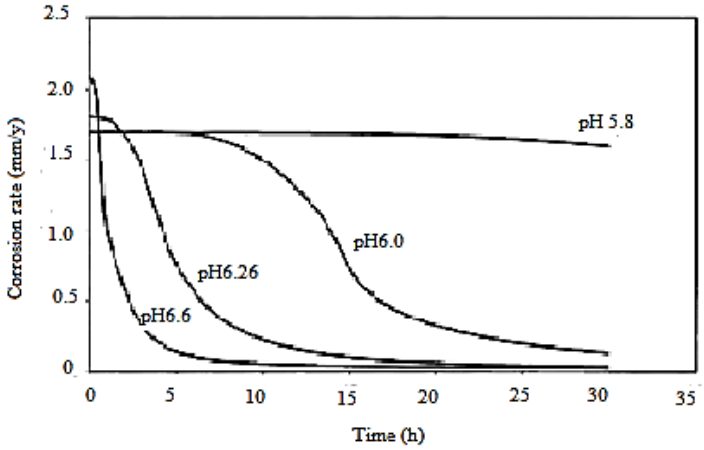

FIGURE 6: Graph of corrosion rate against time at different pH (Srdjan Nesic, 2002)

At pH 5.8, very porous and less protective film was formed which gave almost zero effect to the rate of corrosion. However, a little difference in pH values from 5.8 to 6.0 gave a high impact to the formation of film. At pH 6.0 onwards; denser, thicker and more protective films were formed. The most protective film and great reduction of corrosion rate was at pH 6.6. As the pH was increased more than 5, the probability of film formation increased which led to the decreased of corrosion rate (M. Kermani & Morshed, 2003; Nesic, 2007; Srdjan Nesic, 2002).

CHAPTER 3: METHODOLOGY/PROJECT WORK

3.1 Preparation Of X52 Samples

The type of carbon steel that were used in this project is X52. This metal is classified as low carbon steel because the carbon percentage is lower than 30%. Table 1 shows the composition of X52 based on API 5L X52.

TABLE 1: Composition of X52 Carbon Steel

Composition	**Percentage,%**
Carbon	0.16
Silicon	0.45
Manganese	1.10-1.60
Phosphorus	0.025
Sulphur	0.005
Vanadium	0.05
Niobium	0.20
Titanium	0.02

X52 samples were cut into square shape with dimension of 1 cm (length) x 1 cm (width) x 0.5 cm (height).The samples will then be polished with 120, 240, 360, 480 and 600 grit silicon carbide grinding paper. Next, the samples were rinsed with alcohol and degreased with acetone. Total number of 6 samples needed to be prepared.

3.2 Corrosion Test In Different Fe^{2+} Concentrations at 50°C and 70°C

Each experiment was conducted in a glass cell which is filled with 2 L of distilled water dissolved with 1% wt of sodium chloride (NaCl).The experiments were performed in solution with pH of 6.6 and atmospheric pressure (1 atm). The glass cell was sealed tightly to prevent oxygen contamination, and the CO_2 bubbling was continued throughout the experiment. Table 2 shows the ranges of parameters that were tested in the experiments.

TABLE 2: Range of parameters

Parameters	Value
Fe^{2+} Concentration	0ppm, 50ppm, 200ppm
Temperature	50°C, 70°C

Sodium Hydroxide (NaOH) or hydrogen chloride (HCl) solution were used to adjust to the desired pH. Fe^{2+} concentration was adjusted by using Ferrous Chloride ($FeCl_2$). The duration of each experiment is 48 hours.

3.3 Methods to Measure the Rate of Corrosion and Impedance

3.3.1 Weight Loss Method (WLM)

WLM was conducted based on ASTM G31 to calculate the rate of CO_2 corrosion on X52 samples under different parameters. Firstly, the weight of the samples before immersion were measured. After the test is done for 24 hours, the samples were cleaned and reweighed. The weight loss was be obtained by the subtractions between weight of the sample before and after immersion test. The weight loss was used to calculate the rate of corrosion rate (CR) based on Equation (9), where W is the weight loss, K is a constant, D is the density, A is the exposed area and T is the time of exposure.

$$CR = \frac{W \times K}{D \times A \times T} \qquad (9)$$

3.3.2 Linear Polarization Resistance (LPR)

LPR method was used to measure the rate of corrosion by polarizing the working electrode with $\pm$ 10 mV. Three electrodes were used in this method which are the working electrode, reference electrode and counter electrode. The electrodes were connected to a potentiostat to plot graphs. Graph of current versus potential was plotted and the slope determines the polarization resistance. The polarization resistance is inversely proportional to the rate of corrosion. The corrosion current (I_{corr}) was used to calculate the corrosion rate by using Equation (10), where I_{corr} is the corrosion current, K is a constant, EW is the equivalent weight, D is the density and A is the exposed surface area. This method is referred to ASTM G59-97.

$$CR = \frac{I_{corr}\, K .EW}{dA} \qquad (10)$$

3.3.3 Electrochemical Impedance Spectroscopy (EIS)

This method was used to measure the rate of corrosion. This method uses AC current to find the impedance. The corrosion rate was measured simultaneously with the LPR method. Both EIS and LPR requires the same set up which involves working electrode, reference electrode and counter electrode. The electrodes were connected to a potentiostat. This method is based on ASTM G106-89.

3.4 Methods To Analyse The Morphology Of Film Formation

3.4.1 Scanning Electron Microscope (SEM)

SEM method was used based on ASTM E986 to investigate the morphology of the surfaces of X52 samples. A beam of focused electrons was directed to the sample which then interacted with the atoms to produce various signals. These signals produced SEM images. The images can determine the composition of the sample's surface. This method was done after the immersion test.

3.4.2 Energy Dispersive X-ray Spectroscopy (EDS)

EDS was to analyse the elemental composition and chemical characterization of a sample. X-Rays was directed to the sample and this will result in set of X-Ray emission spectrum for each element. When the X- Rays beam is focus on the area where film or corrosion product are formed, it can determine the types of element of the film. This method is based on ASTM F1375 – 92.

3.5 Key Milestone

3.6 Gantt Chart for Final Year Project 1

Number	Detail / Week	1	2	3	4	5	6	7	8	9	10	11	12	13	14
1	FYP Briefing with Coordinator	■													
2	Topic Introduction with SV		■												
3	Discussion with SV about the project			■	■	■	■	■	■	■	■	■	■	■	
4	Research on Relevant References			■	■	■	■	■	■	■	■	■	■		
5	Summarized research papers			■	■	■	■	■	■	■	■	■	■		
6	Prepare Extended Proposal						■	■							
7	Extended Proposal Submission							▲							
8	Proposal Defence										▲				
9	Prepare Interim Report									■	■	■	■	■	
10	Interim Report Submission														▲

3.7 Gantt Chart for Final Year Project 2

Number	Detail / Week	1	2	3	4	5	6	7	8	9	10	11	12	13	14	15
1	Preparation of Samples	■														
2	Corrosion Test in different pH, Temperature and Fe2+		■	■	■	■	■	■								
3	Rate of CO_2 Corrosion and Film Morphology		■	■	■	■	■	■								
4	Preparation of Progress Report			■	■	■	■	■								
5	Submission of Progress Report							▲								
6	Pre-Sedex										▲					
7	Preparation of Draft Final Report							■	■	■	■	■				
8	Submission of Draft Final Report											▲				
9	Submission of Dissertation												▲			
10	Submission of Technical Paper												▲			
11	Viva													▲		
12	Submission of Project Dissertation															▲

▲ Indicates the key milestone of the project

■ Process

CHAPTER 4: RESULTS AND DISCUSSION

4.1 Weight Lost Method (WLM)

WLM results at 0 ppm, 50 ppm and 100 ppm Fe^{2+} concentration at 50°C and 70°C after 48 hours were obtained as in Fig.7 and 8 respectively. Fig. 9 shows the comparison between both results at 50°C and 70°C. Based on Figure 9, at 0 ppm, the corrosion rate at 70°C, 1.92mm/yr is higher compared to 50°C which is 1.15mm/yr. As the temperature increased, the corrosion rate increased. However, at 50ppm, both corrosion rate for 50°C and 70°C decreased to 0.95mm/yr and 1.13mm/yr respectively due to formation of film on steel surfaces. At 200 ppm, the corrosion rate at 70°C, 0.44mm/yr tend to be lower than 50°C, 0.64mm/yr which means that better film was formed at 70°C. These results showed that even though the corrosion rate increased at higher temperature, increased in Fe^{2+} concentrations can effectively lowered down the corrosion rate.

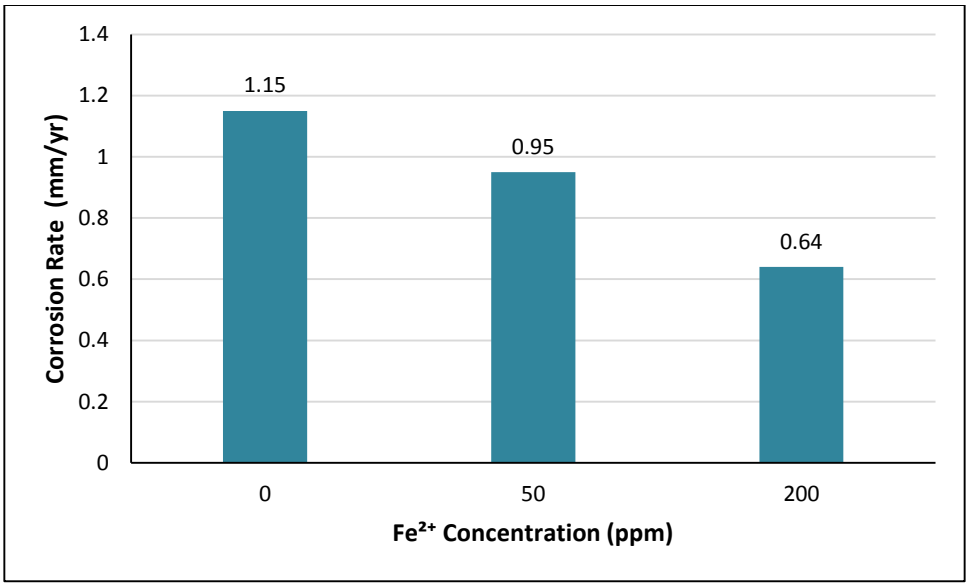

FIGURE 7: WLM Corrosion Rate vs Fe^{2+} Concentration at 50°C

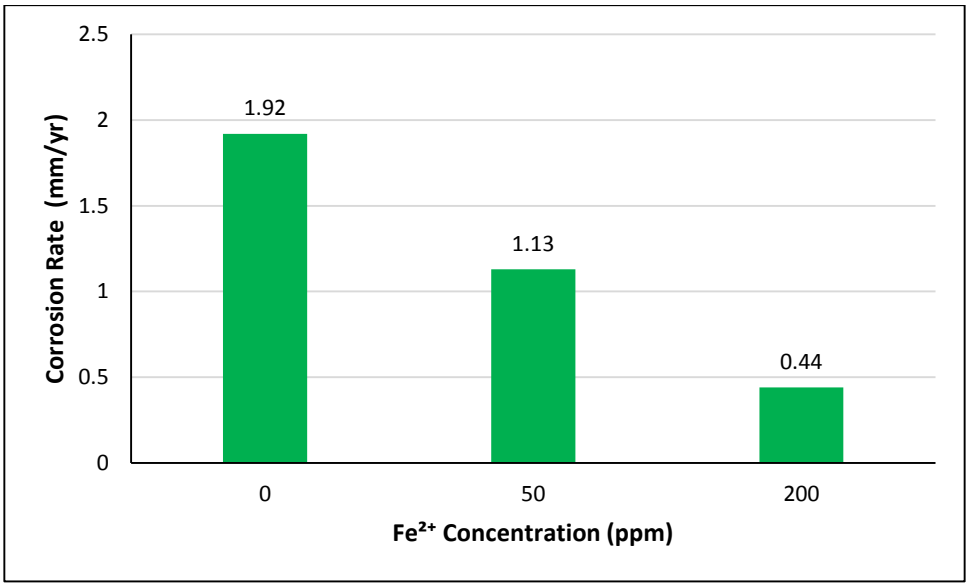

FIGURE 8: WLM Corrosion Rate vs Fe^{2+} Concentration at 50°C

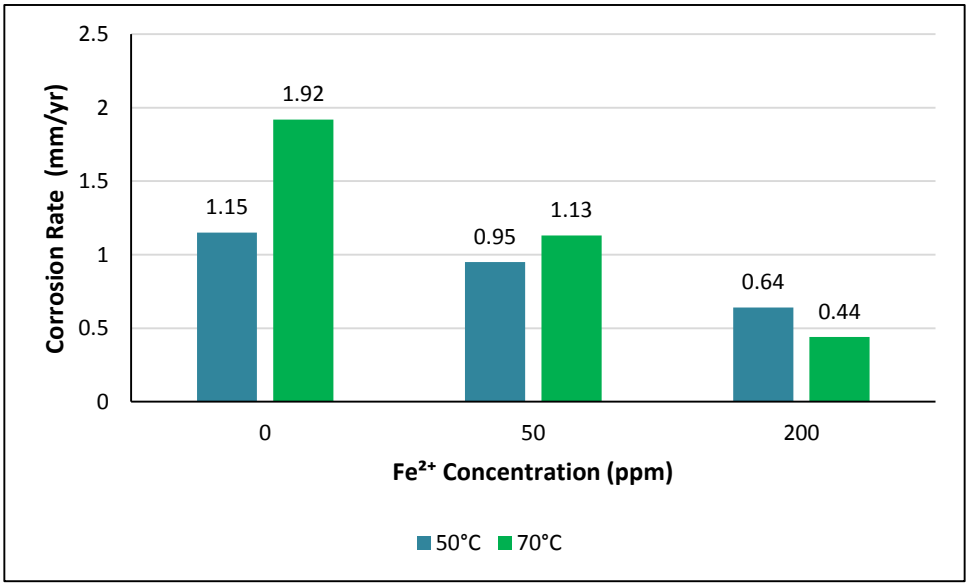

FIGURE 9: WLM Corrosion Rate vs Fe^{2+} Concentration at 50°C and 70°C

4.2 Linear Polarization Resistance (LPR)

LPR was used to measure the corrosion rate at an interval duration of 1 hour for 48 hours. Fig. 10 and 11 shows the results of LPR corrosion at every hour at 50°C and 70°C with different Fe^{2+} concentrations. At 0 ppm, for both 50°C and 70°C, the values of corrosion rate were alternately went up and down. These explained that as the corrosion rate decreased, film started to form. However, detached of film was the reason for the increased of corrosion rates. At 50 ppm, when the temperature is 50°C, the corrosion rates changed slightly through 48 hours which means that very less protective film was formed. However, the corrosion rates at 70°C decreased through 48 hours. At 200 ppm, the corrosion rate after 48 hours for 70°C, 1mm/yr is lesser than corrosion rate at 50°C, 1.35mm/yr. This shows that the film formed on the surface at 70°C was thicker and better resistance against corrosion.

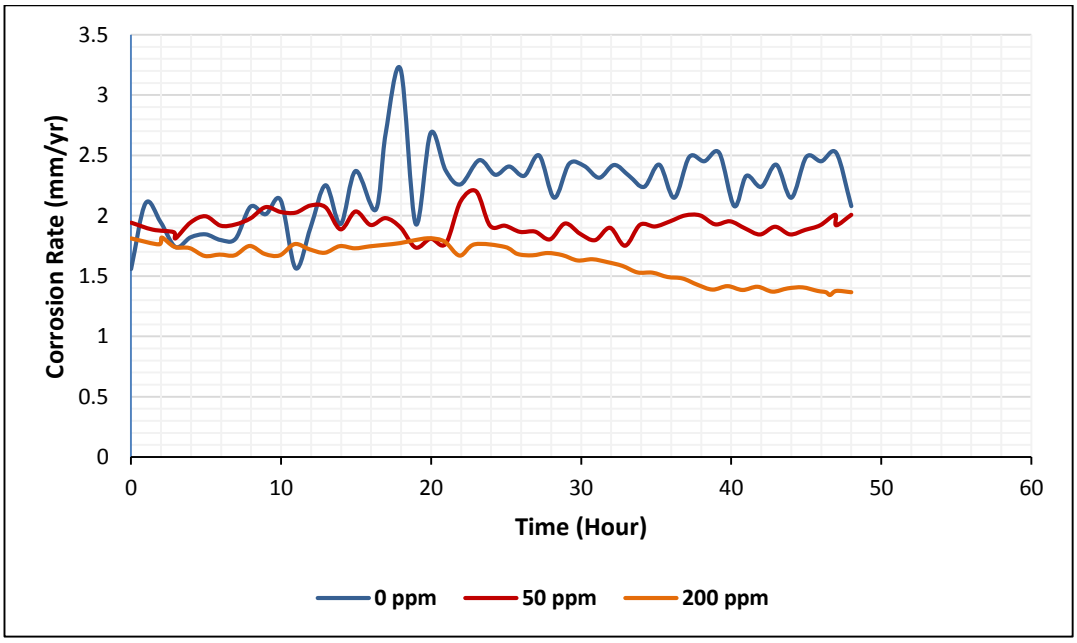

FIGURE 10: LPR Corrosion Rate vs Time at 50°C

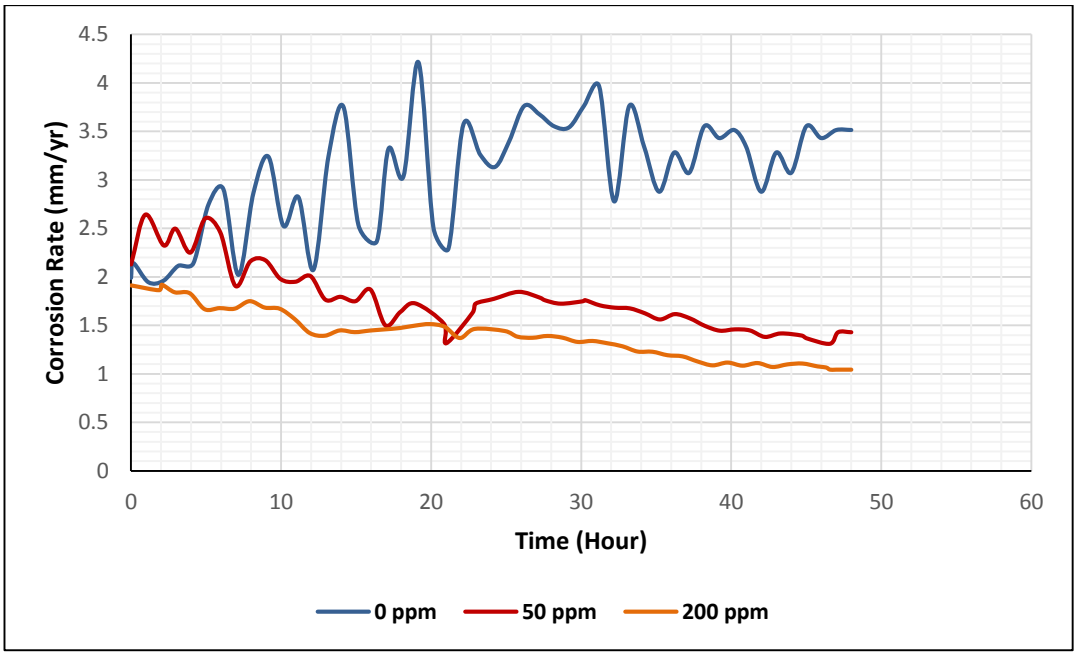

FIGURE 11: LPR Corrosion Rate vs Time at 70°C

TABLE 3: WLM and LPR Corrosion Rate At Different Temperature And Fe^{2+} Concentration

Temperature (°C)	Fe^{2+} concentration	WLM Corrosion Rate (mm/yr)	Average of LPR Corrosion Rate (mm/yr)
50	0	1.15	2.23
	50	0.95	1.93
	200	0.64	1.61
70	0	1.92	3.05
	50	1.13	1.77
	200	0.44	1.39

Table 3 shows the results of WLM and average of LPR corrosion rates for different Fe^{2+} concentrations at 50°C and 70°C.At 0 ppm, both WLM and average of LPR corrosion rates at 70°C were higher as compared to 50°C. However, the corrosion rates at 70°C with 200 ppm are lower as compared to 50°C with 200 ppm. These show that film formation is more favourable in 70°C as the Fe^{2+} concentrations increases.

4.3 Electrochemical Impedance Spectroscopy (EIS)

The diameter of Nyquist semicircles and impedance values of Bode Plots can determine the presence of film on the steel surface. The results were measured at 0 , 24 and 48 hours respectively. Based on Fig.12-14, as the Fe^{2+} concentrations increased at 50°C, the diameter of semicircles increased followed by the impedance values for 0 , 24 and 48 hours. The results for 70°C can be referred to Fig. 15-17. It can be observed that the largest diameter of semicircle and highest value of impedance was at 70°C with 200 ppm after 48 hours which means that most protective film was formed at this condition.

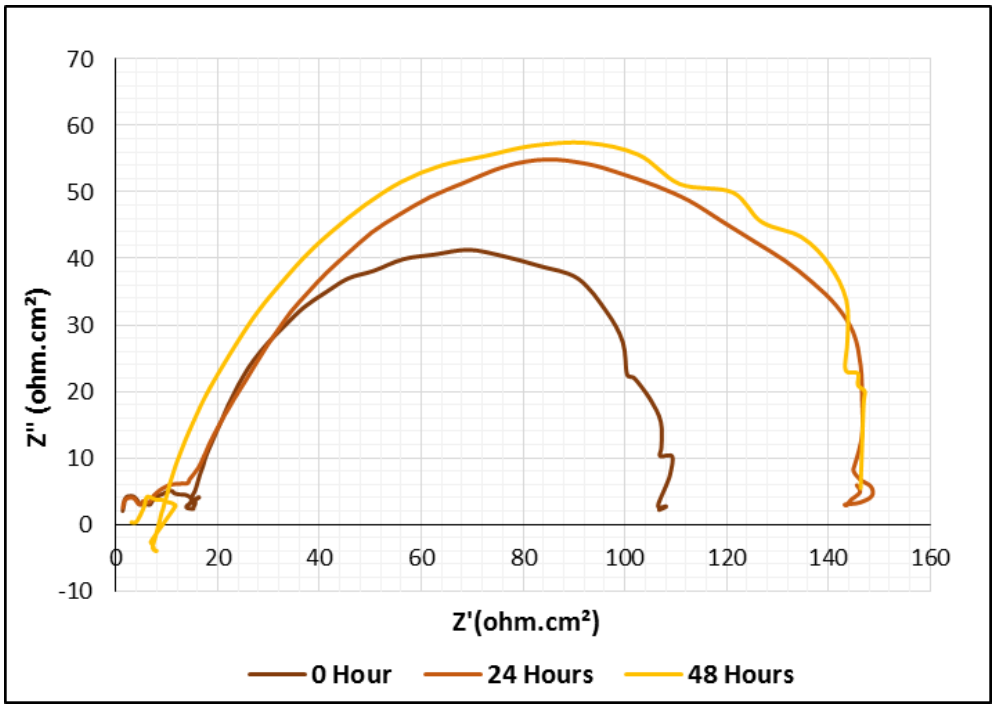

a)

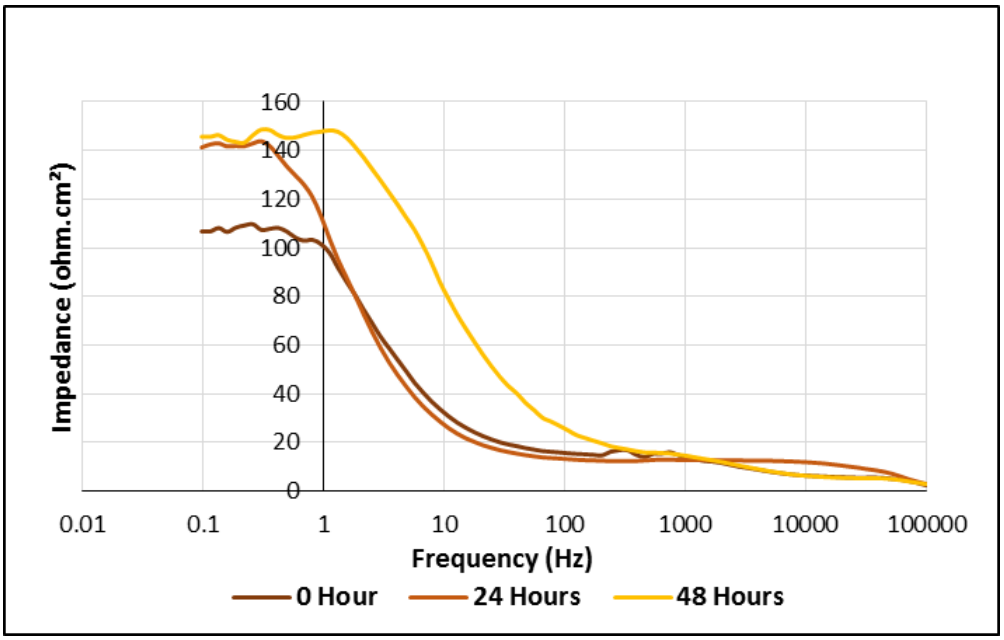

b)

FIGURE 12: EIS at 50°C and 0 ppm a) Nyquist Plot b) Bode Plot

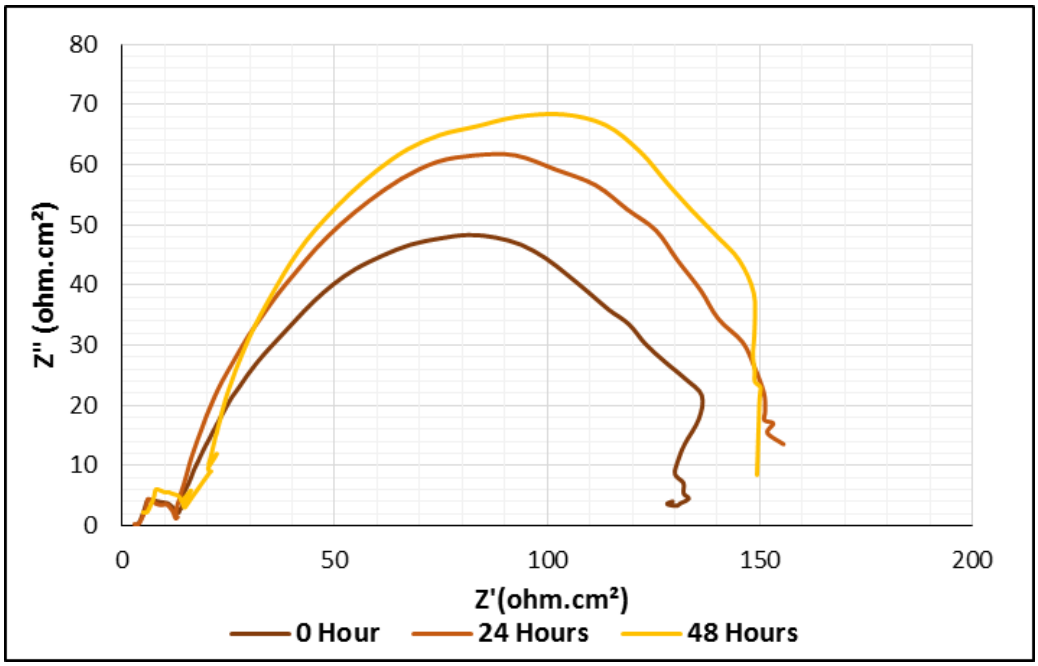

a)

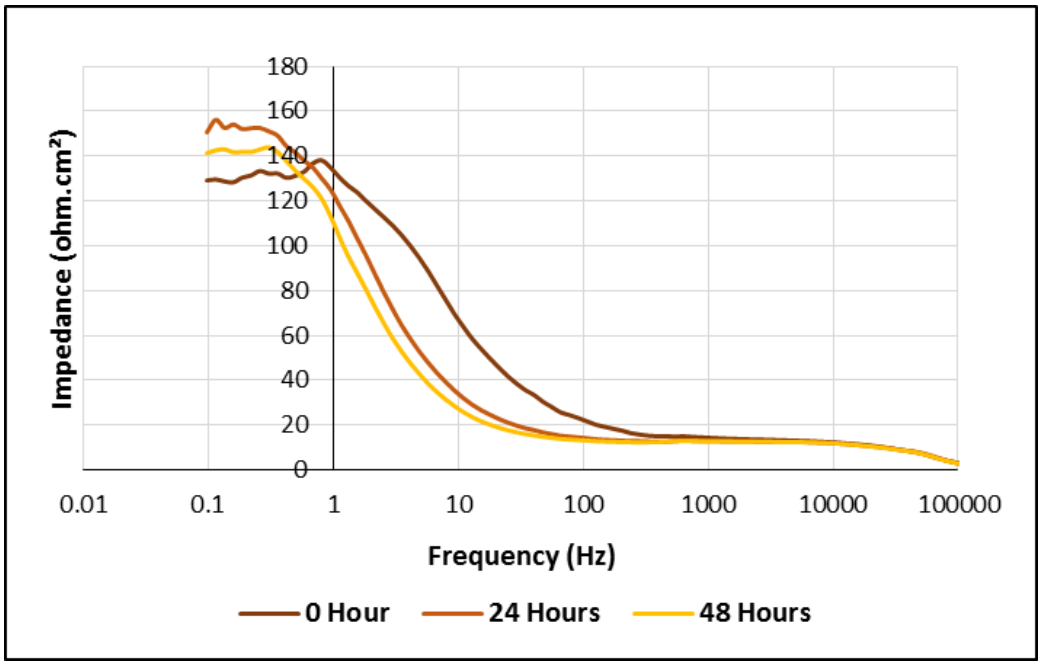

b)

FIGURE 13: EIS at 50°C and 50 ppm a) Nyquist Plot b) Bode Plot

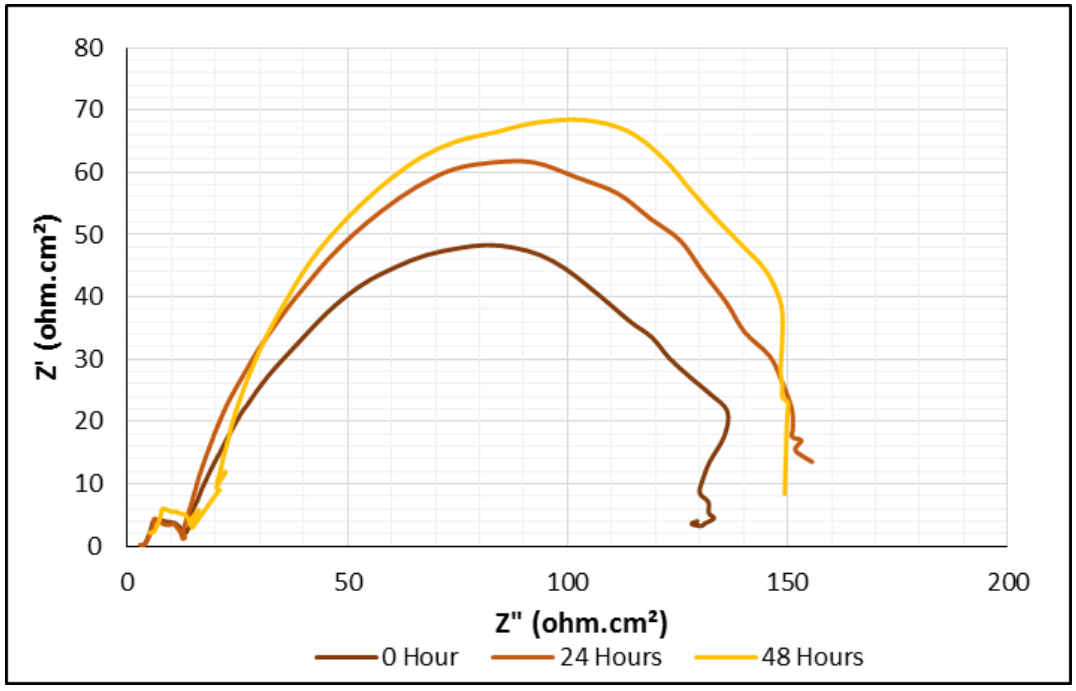

a)

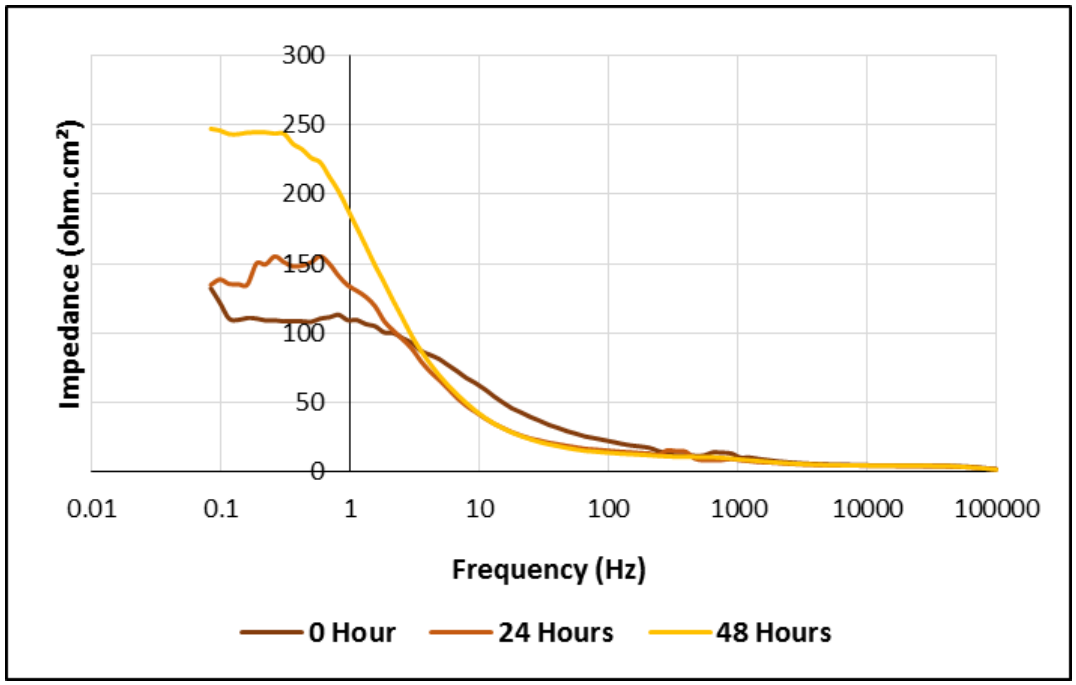

b)

FIGURE 14: EIS at 50°C and 200 ppm a) Nyquist Plot b) Bode Plot

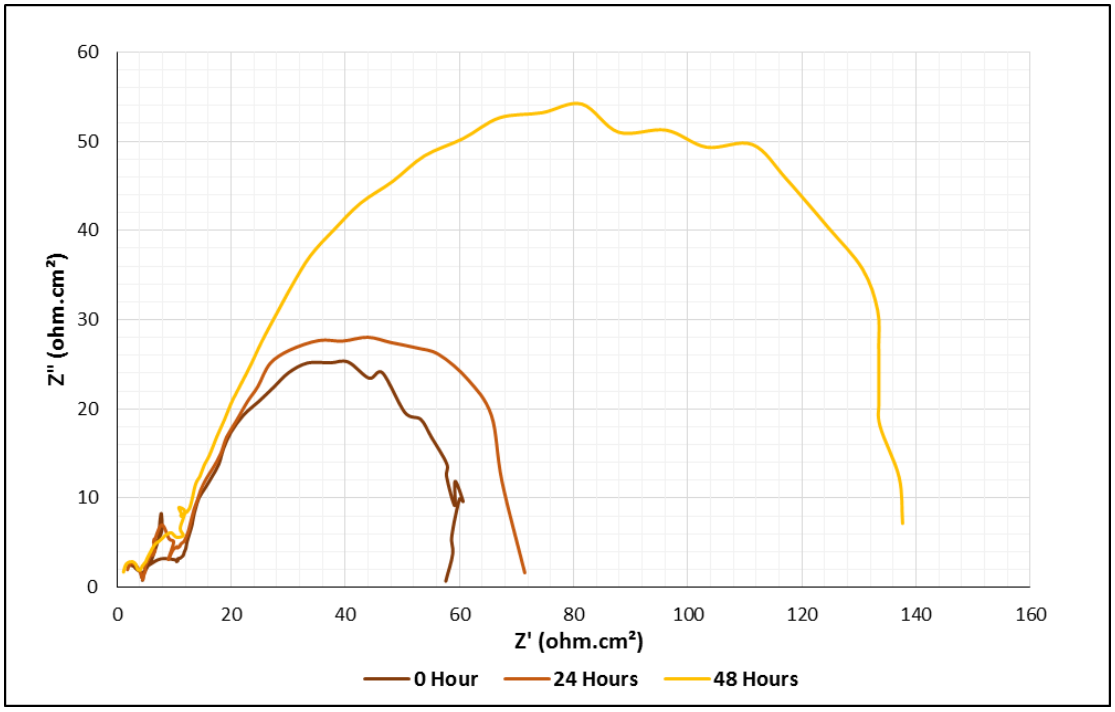

a)

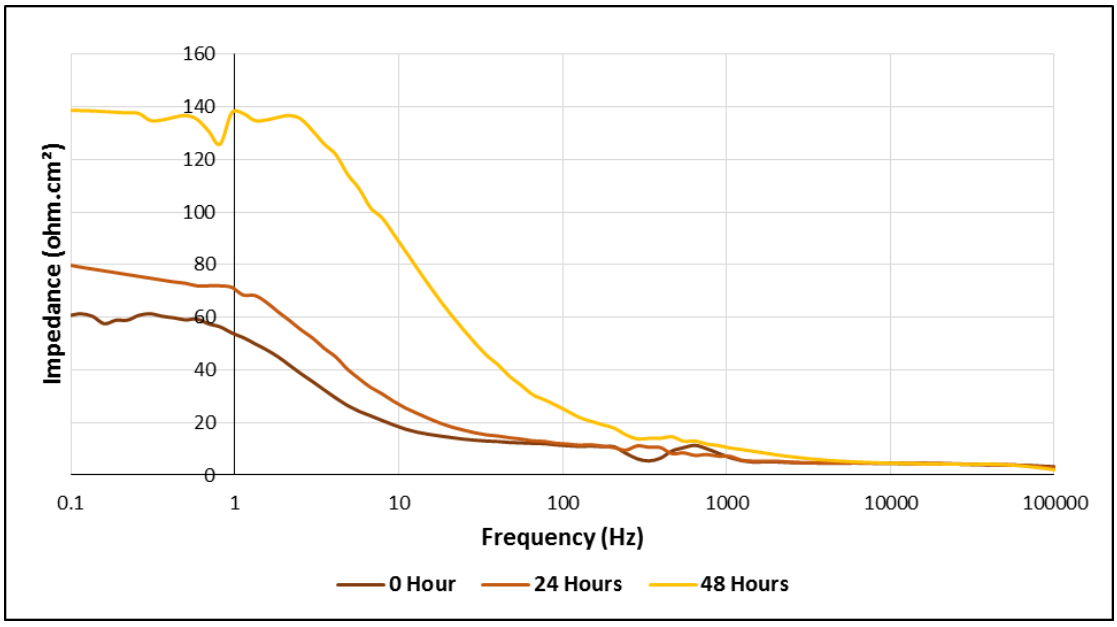

b)

FIGURE 15: EIS at 70°C and 0 ppm a) Nyquist Plot b) Bode Plot

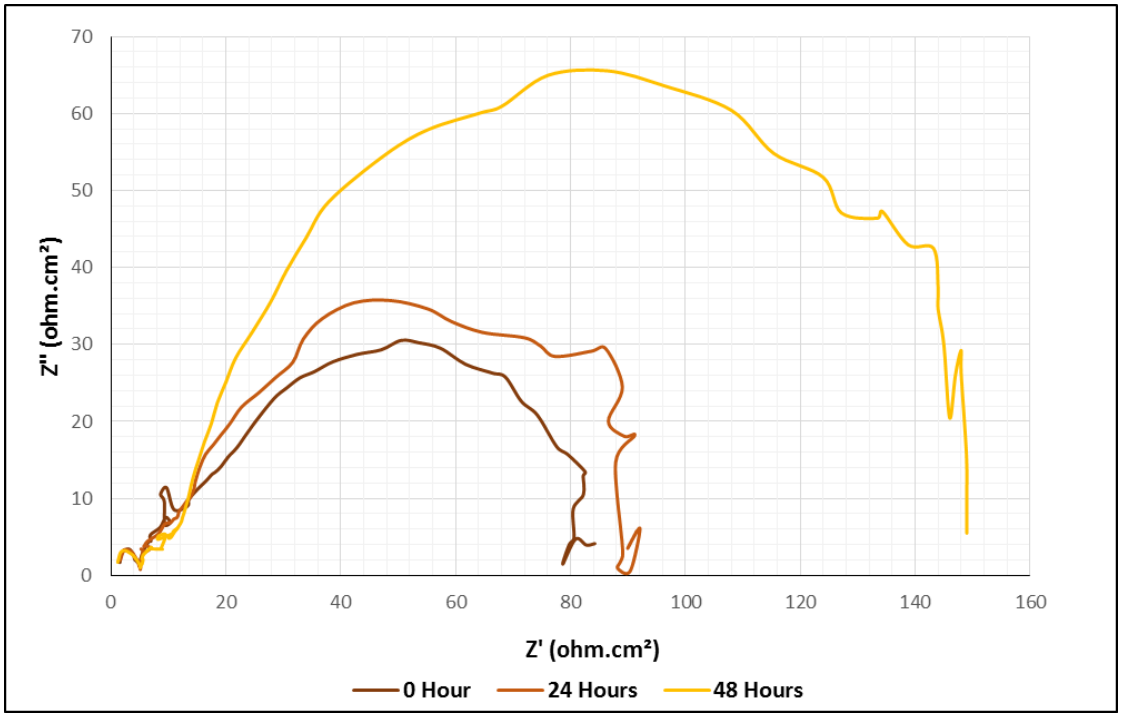

a)

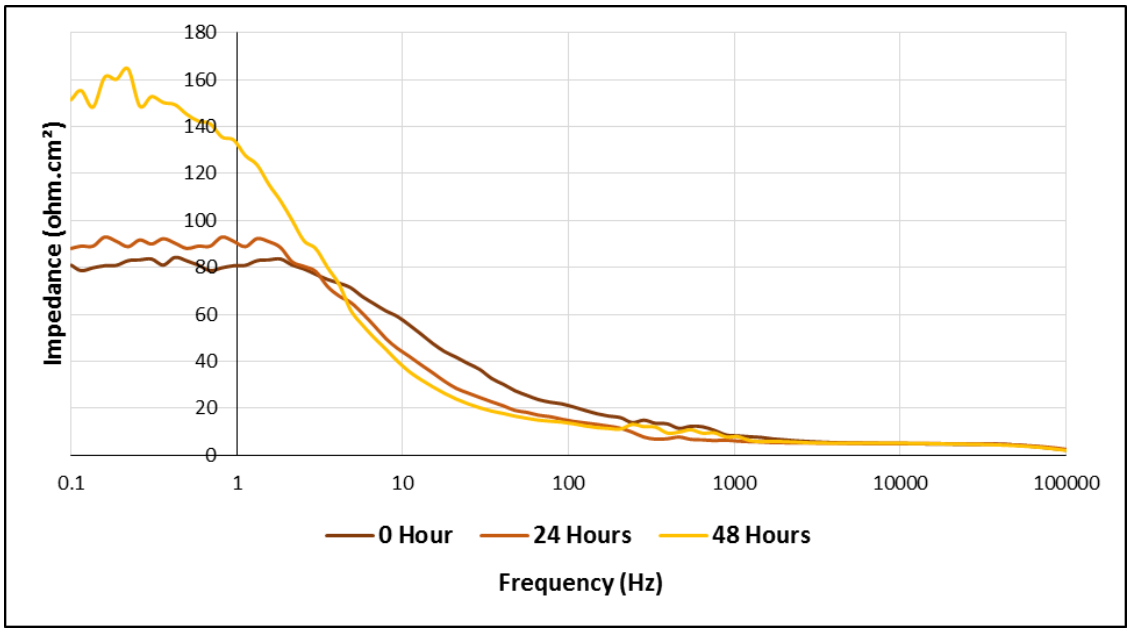

b)

FIGURE 16: EIS at 70°C and 50 ppm a) Nyquist Plot b) Bode Plot

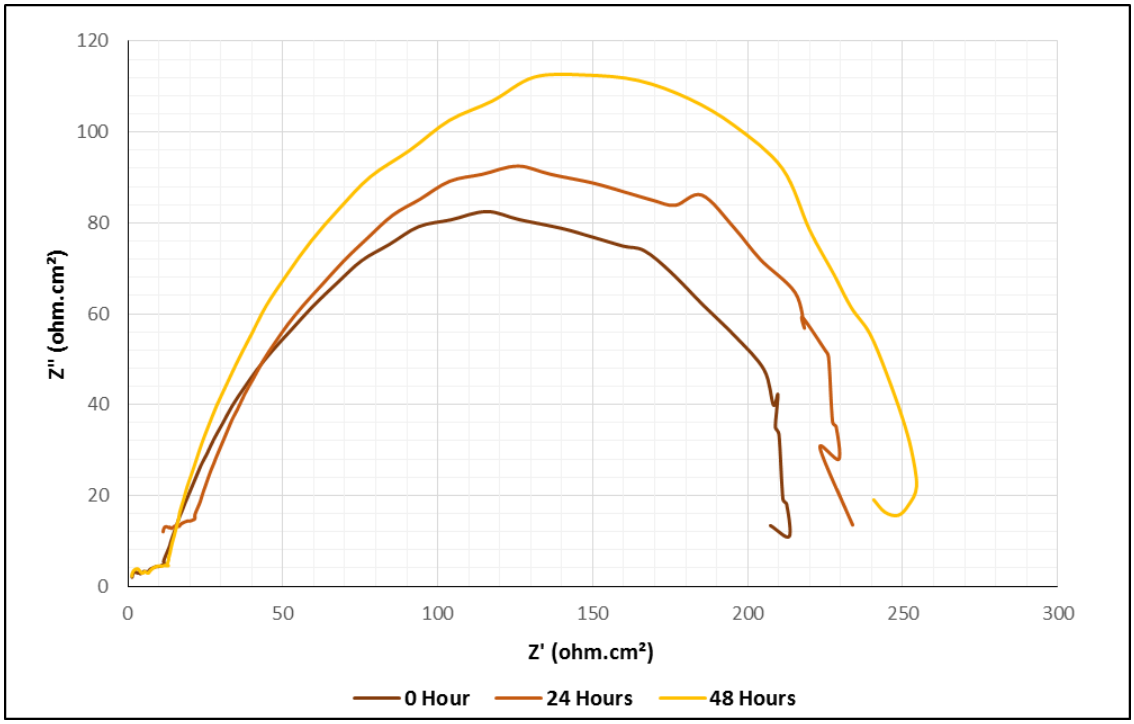

a)

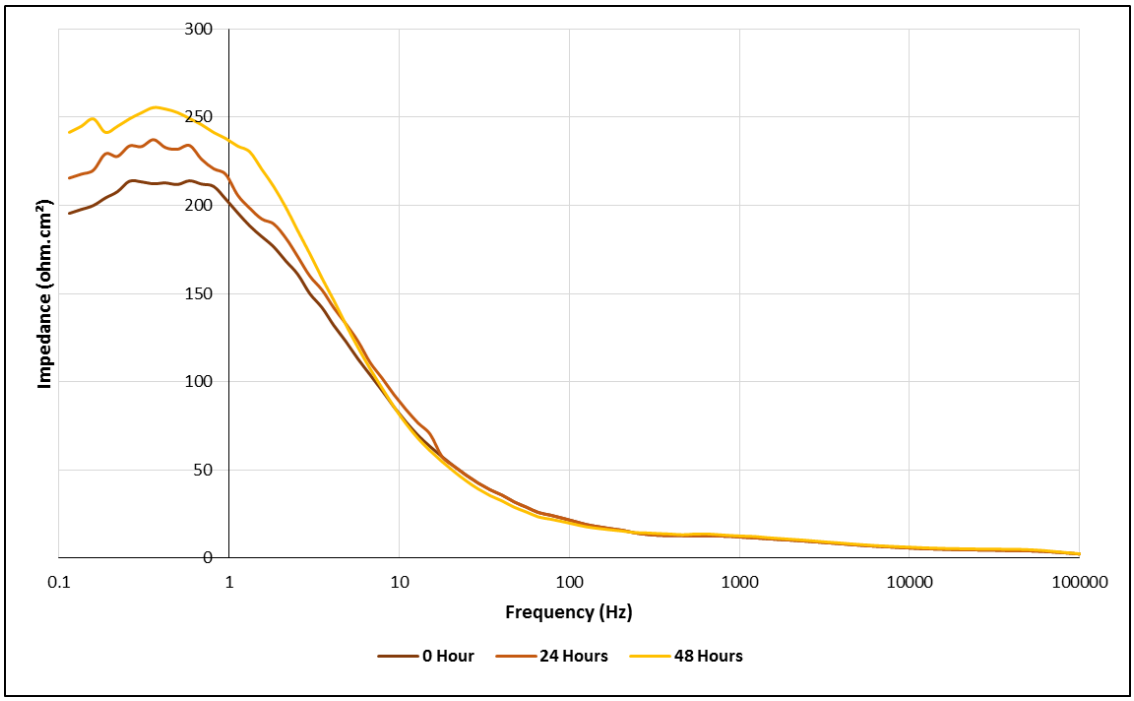

b)

FIGURE 17: EIS at 70°C and 200 ppm a) Nyquist Plot b) Bode Plot

4.4 Scanning Electron Microscopy (SEM)

SEM images were observed from four different samples with three magnifications as in Fig. 18-21. The crystals are most likely to be $FeCO_3$ precipitates. Based on Fig.18, very less crystals were formed on the surface at 50°C with 50 ppm which resulted in less resistance against corrosion. At 50°C with 200 ppm as in Fig.19, more $FeCO_3$ precipitates were observed but it did not create a protective film against corrosion. From Fig.20, it can be observed that more $FeCO_3$ precipitates were formed at 70°C with 50 ppm. The film formed can reduced the rate of corrosion better as compared to Fig. 19 and 20. The most protective film formed can be observed from Fig. 21 at 70°C with 200 ppm. The film was very compact and this prevented other corrosion species to react with the underneath surface which greatly reduced the rate of corrosion.

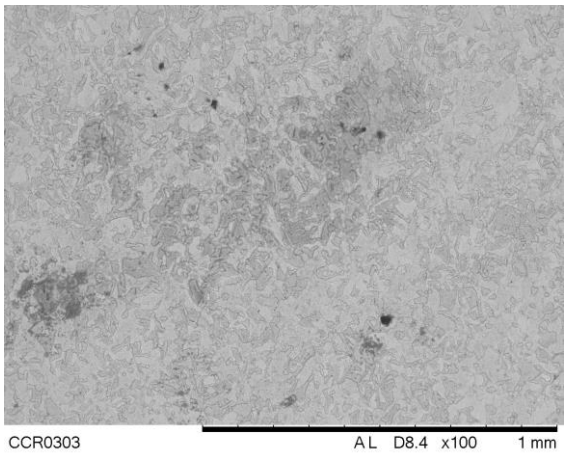

a)

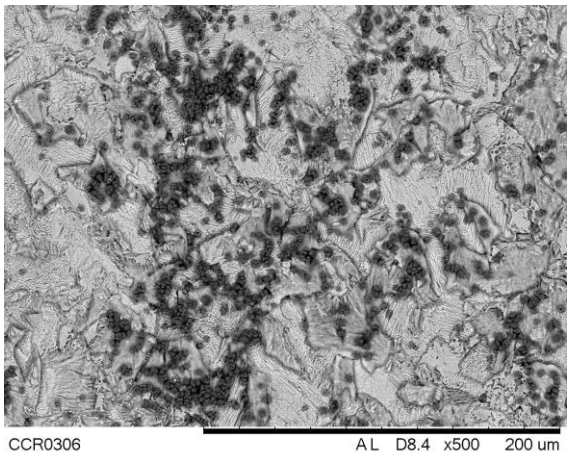

b)

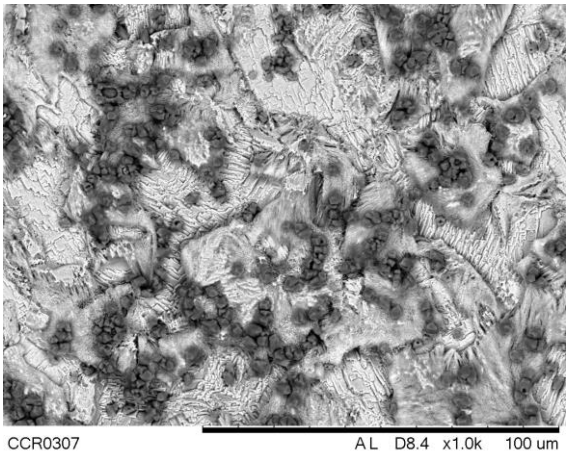

c)

FIGURE 18: SEM Morphologies At 50°C With 50 ppm Fe^{2+}Concentration At Different Magnifications a) X100 b) X500 c) X1000

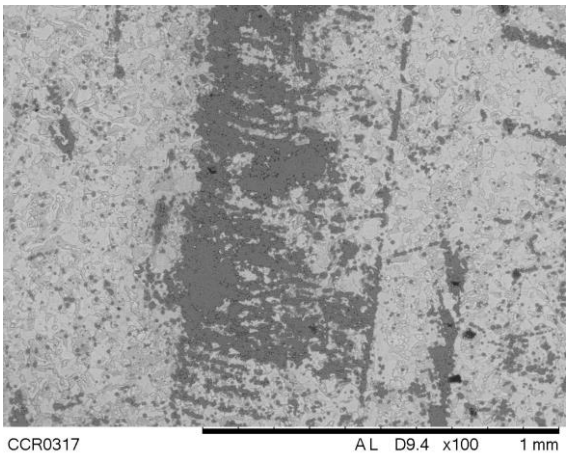

a)

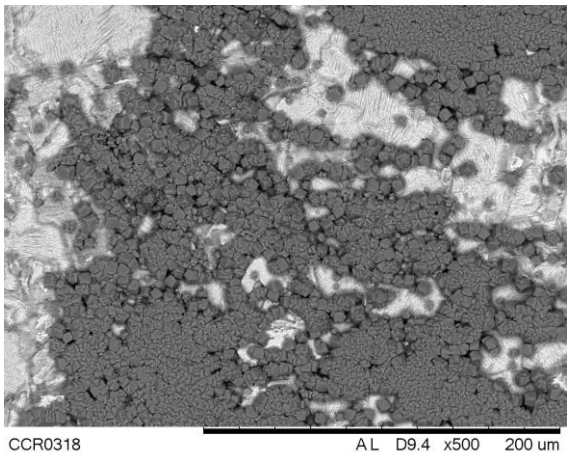

b)

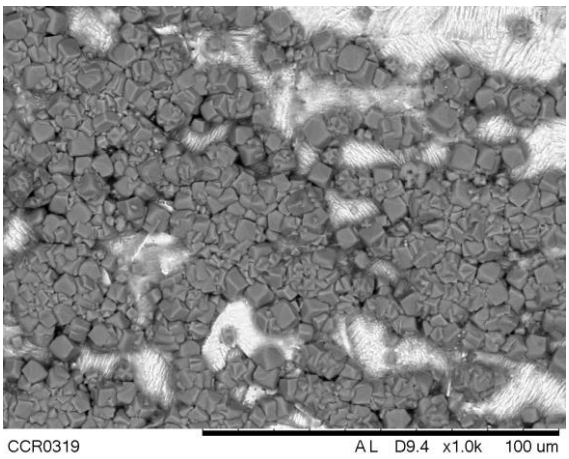

c)

FIGURE 19: SEM Morphologies At 50°C With 200 ppm Fe^{2+}Concentration At Different Magnifications a) X100 b) X500 c) X1000

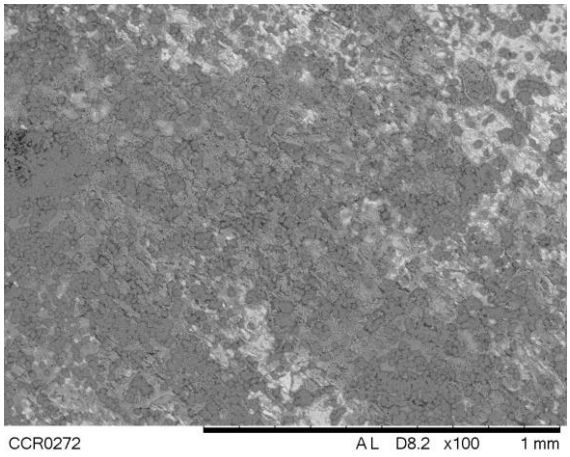

a)

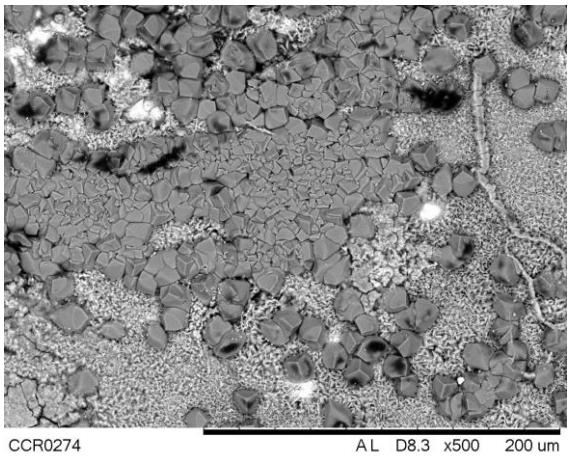

b)

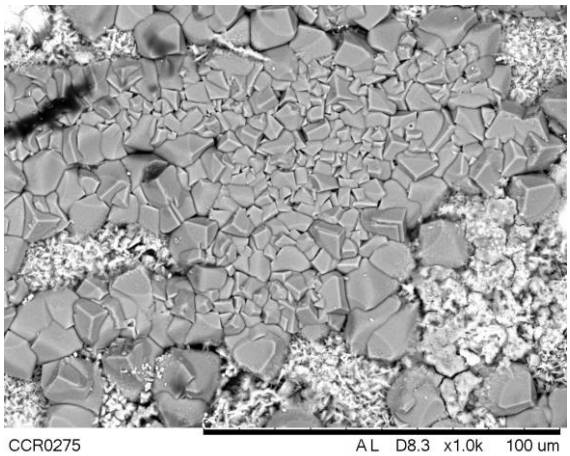

c)

FIGURE 20: SEM Morphologies At 70°C With 50 ppm Fe^{2+}Concentration At Different Magnifications a) X100 b) X500 c) X1000

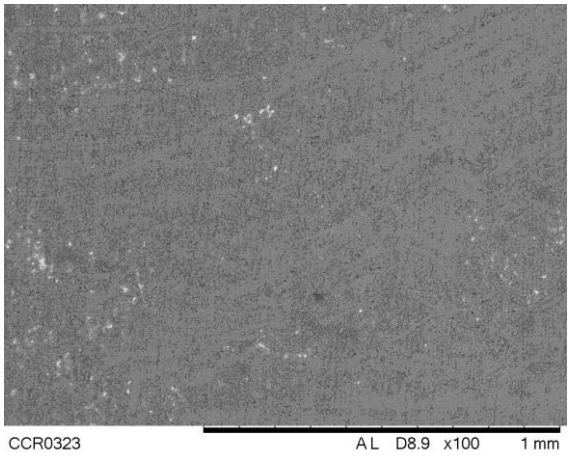

a)

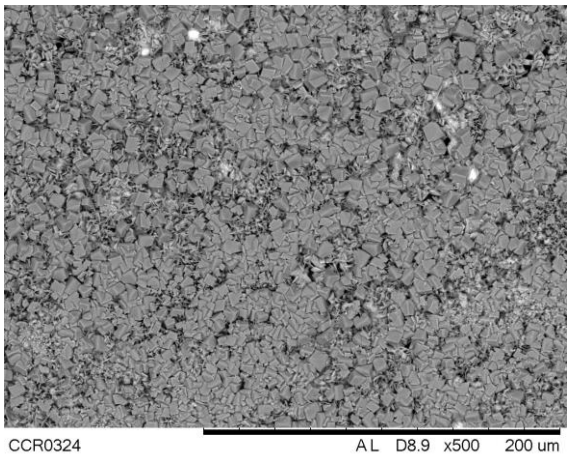

b)

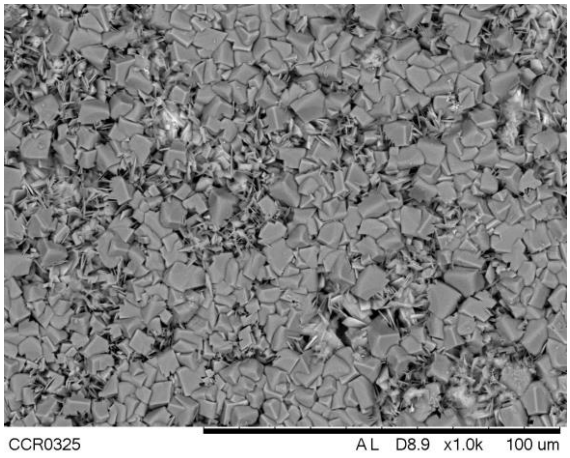

c)

FIGURE 21: SEM Morphologies At 70°C With 200 ppm Fe^{2+}Concentration At Different Magnifications a) X100 b) X500 c) X1000

4.5 Energy Dispersive X-ray Spectroscopy (EDS)

EDS patterns were obtained as in Fig. 22-25 to determine the composition of elements on the steel surface. There are three different elements which are Iron (Fe), Oxygen (O) and Carbon (C). The amount of $FeCO_3$ can be determine by these three elements. As the number of $FeCO_3$ increases, Fe will decreases while both O and C will increase. The highest amount of Fe and lowest amount of both O and C was obtained at 50°C with 50 ppm as in Fig. 22 where very less $FeCO_3$ can be observed. Conversely, the least amount of Fe and highest amount of both O and C can be obtained at 70°C with 200 ppm as in Fig. 25 where most $FeCO_3$ can be observed.

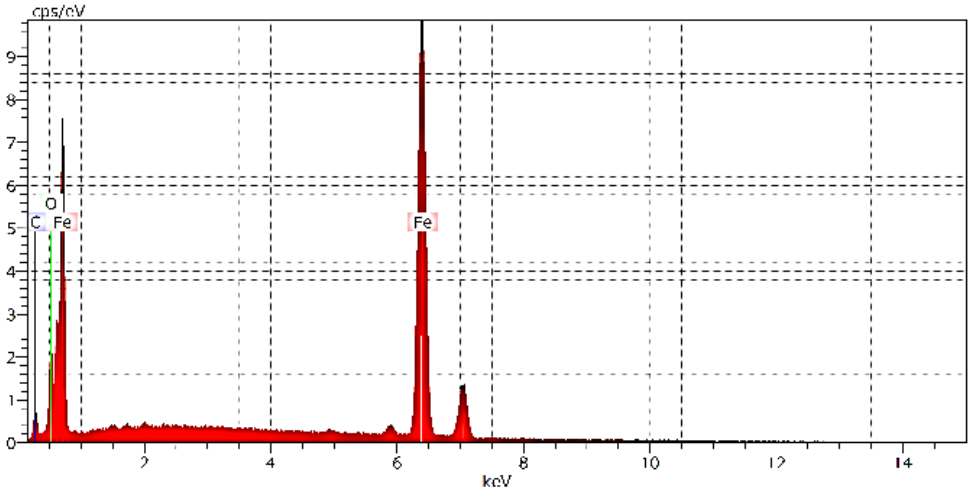

Spectrum: Point

Element	AN	Series	norm. C [wt.%]	Atom. C [at.%]
Iron	26	K-series	90.28	69.61
Oxygen	8	K-series	4.97	13.37
Carbon	6	K-series	4.75	17.02
		Total:	100.00	100.00

FIGURE 22: EDS Pattern at 50°C with 50 ppm Fe^{2+} Concentration

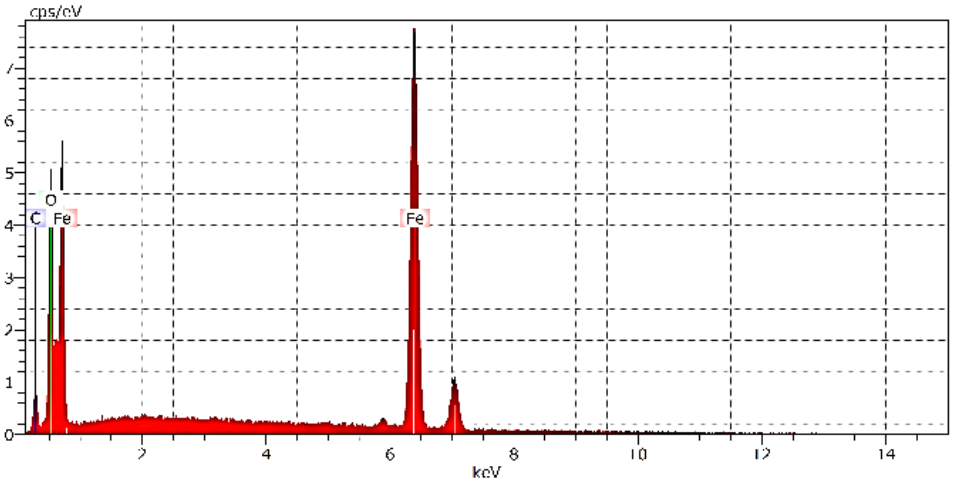

Spectrum: Point

Element	AN	Series	norm. C [wt.%]	Atom. C [at.%]
Iron	26	K-series	78.65	48.95
Oxygen	8	K-series	14.90	32.37
Carbon	6	K-series	6.45	18.67
		Total:	100.00	100.00

FIGURE 23: EDS Pattern at 50°C with 200 ppm Fe^{2+} Concentration

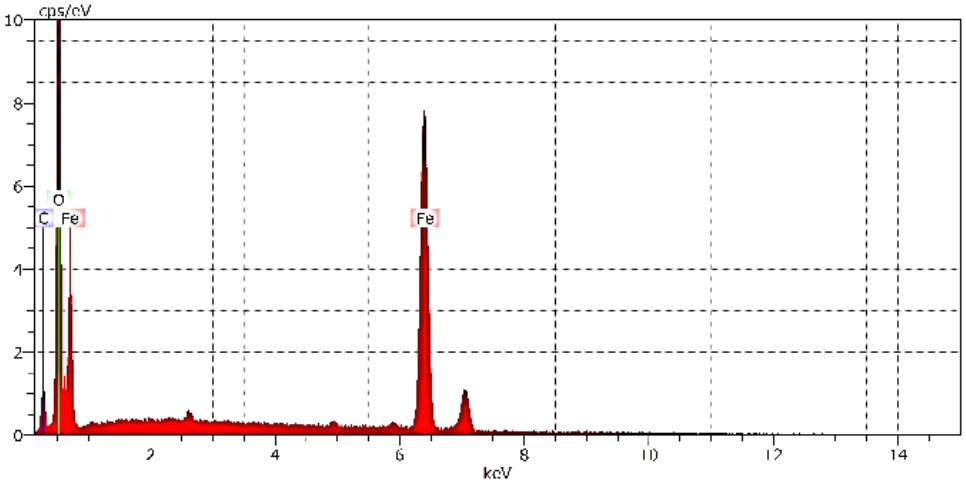

Spectrum: Point

Element	AN	Series	norm. C [wt.%]	Atom. C [at.%]
Iron	26	K-series	63.12	31.61
Oxygen	8	K-series	30.10	52.62
Carbon	6	K-series	6.77	15.77
		Total:	100.00	100.00

FIGURE 24: EDS Pattern at 70°C with 50 ppm Fe^{2+} Concentration

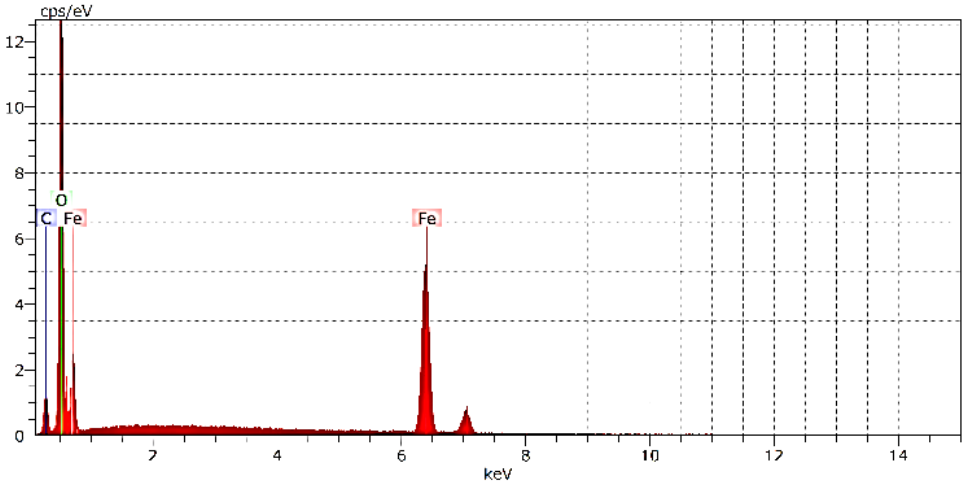

Spectrum: Point

Element	AN	Series	norm. C [wt.%]	Atom. C [at.%]
Iron	26	K-series	52.45	22.97
Oxygen	8	K-series	38.97	59.56
Carbon	6	K-series	8.58	17.47
Total:			100.00	100.00

FIGURE 25: EDS Pattern at 70°C with 200 ppm Fe^{2+} Concentration

CHAPTER 5: CONCLUSION AND RECOMMENDATION

5.1 Conclusion

Based on the results obtained, the objective which is to study the effect of Fe^{2+} concentrations on the rate of CO_2 corrosion on X52 steel at 50°C and 70°C has been achieved. The rate of corrosion rate at 70°C is higher as compared to 50°C in CO_2 environment at 0 ppm. In addition, the both results did not show the presence of film due to no constant drop of corrosion rates. At Fe^{2+} concentration of 50 ppm, decreased of corrosion rates were observed for both 50°C and 70°C. However, better protective film was formed at 70°C as compared to 50°C. This shows that the formation of film is more favourable at 70°C.

Better agreement to determine that film formation is better at 70°C can be obtained when the Fe^{2+} concentration is 200 ppm. The number of $FeCO_3$ precipitates is higher as compared to 50°C which created a very protective film which regularly decreased the corrosion rate. Therefore, Fe^{2+} concentration plays an important role in decreasing the rate of corrosion. Temperature is also important to provide a favourable temperature for the development of a protective film.

5.2 Recommendation

More SEM and EDS images are needed to have better comparisons between different Fe^{2+} concentrations and temperatures. Due to time constraint, the unsuccessful results for 100 ppm at 50°C and 70°C were no repeated. More time is needed so that more results can be compared and discussed. Other than that, more parameters such as pressure and velocity are needed to be controlled to get the best results as in the actual environment of corrosion in pipeline.

X-Ray Diffraction (XRD) is recommended to be used to observe the composition of compound of the corrosion products form on the steel surface. $FeCO_3$ a better corrosion product to form a very compact and protective film as compared to Iron Carbide (Fe_3C).This method can analyse the presence of which type of corrosion product on the steel surface which helps to get better agreement whether the film is made out of $FeCO_3$.

REFERENCES

Cabrini, M., Lorenzi, S., Pastore, T., & Radaelli, M. (2015). Corrosion rate of high CO2 pressure pipeline steel for carbon capture transport and storage. *La Metallurgia Italiana*(6).

Clover, D., Kinsella, B., Pejcic, B., & De Marco, R. (2005). The influence of microstructure on the corrosion rate of various carbon steels. *Journal of applied electrochemistry, 35*(2), 139-149.

Dugstad, A. (2006). *Fundamental aspects of CO2 metal loss corrosion-part 1: mechanism.* Paper presented at the CORROSION 2006.

El-Lateef, H. A., Abbasov, V. M., Aliyeva, L. I., & Ismayilov, T. A. (2012). Corrosion protection of steel pipelines against CO 2 corrosion—a review. *Chem. J, 2*(2), 52-63.

Fang, H., Brown, B., & Nešic, S. (2013). Sodium Chloride Concentration Effects on General CO2 Corrosion Mechanisms. *Corrosion, 69*(3), 297-302.

Kermani, B., Martin, J. W., & Esaklul, K. A. (2006). *Materials design strategy: effects of H2S/CO2 corrosion on materials selection.* Paper presented at the CORROSION 2006.

Kermani, M., & Morshed, A. (2003). Carbon dioxide corrosion in oil and gas production-A compendium. *Corrosion, 59*(8), 659-683.

Li, T., Yang, Y., Gao, K., & Lu, M. (2008). Mechanism of protective film formation during CO 2 corrosion of X65 pipeline steel. *Journal of University of Science and Technology Beijing, Mineral, Metallurgy, Material, 15*(6), 702-706.

Nesic, S. (2007). Key issues related to modelling of internal corrosion of oil and gas pipelines–A review. *Corrosion Science, 49*(12), 4308-4338.

Nesic, S., Wang, S., Cai, J., & Xiao, Y. (2004). *Integrated CO2 corrosion-multiphase flow model.* Paper presented at the SPE International Symposium on Oilfield Corrosion.

Schmitt, G., & Horstemeier, M. (2006). *Fundamental aspects of CO2 metal loss corrosion-Part II: Influence of different parameters on CO2 corrosion mechanisms.* Paper presented at the CORROSION 2006.

Srdjan Nesic, K.-L. J. L. a. V. R. (2002). *A MECHANISTIC MODEL OF IRON CARBONATE FILM GROWTH AND THE EFFECT ON CO2 CORROSION OF MILD STEEL* Paper presented at the CORROSION 2002.

Sun, W., Nesic, S., & Papavinasam, S. (2006). Kinetics of iron sulfide and mixed iron sulfide/carbonate scale precipitation in CO2/H2S corrosion. *Corrosion/2006, paper*(6644).

Tang, X., Li, C., Ayello, F., Cai, J., Nesic, S., Cruz, C. I. T., & Al-Khamis, J. N. (2007). Effect of oil type on phase wetting transition and corrosion in oil-water flow. *Proceedings of the Corrosion, 7*.

Tanupabrungsun, T., Brown, B., & Nesic, S. (2013). *Effect of pH on CO2 Corrosion of Mild Steel at Elevated Temperatures.* Paper presented at the CORROSION/2013 NACE INTERNATIONAL Conference & Expo. Ohio University.

Uzorh, E. D. A. C. (2013). Corrosion Properties of Plain Carbon Steels. *The International Journal Of Engineering And Science (IJES), 2*(11), 18-24.